APPLIED ORGANOMETALLIC CHEMISTRY
Appl. Organometal. Chem. 2001; **15**: 414–420
DOI: 10.1002/aoc.163

Synthesis, and structural and morphological characterization of iron oxide–ion-exchange resin and –cellulose nanocomposites†

Lorenza Suber,[1]* Sabrina Foglia,[1] Gabriel Maria Ingo[1] and Nikos Boukos[2]
[1]ICMAT–CNR, Area della Ricerca di Roma, Via Salaria km 29,300, 00016, Monterotondo St., Rome, Italy
[2]Institute of Materials Science, National Center for Scientific Research, "Demokritos", POB 60228, Athens, Greece

The synthesis and the comparative structural and morphological study of iron oxide nanoparticles in polystyrene-based ion-exchange resins and cellulosics are reported. The synthesis of magnetite was performed under nitrogen atmosphere by an *in situ* method in the presence of the matrix itself. Scanning and transmission electron microscopy measurements led to a detailed characterization of matrix morphology and of magnetic particle structure, size and morphology. The results show that the matrix influences the iron oxide particle size; the average size is about 7 nm in the resins and 25 nm in the celluloses. In the resins, particles are present inside the pores and as aggregates on the surface of the resin beads, whereas in the cellulose they are present on the surface and in the swollen network of the microfibers constituting the single fibers. Copyright © 2001 John Wiley & Sons, Ltd.

Keywords: magnetite nanoparticles; maghemite nanoparticles; magnetic nanocomposite

INTRODUCTION

Technological progress is dependent on materials possessing new or enhanced properties. Few pure materials have all the physical and mechanical properties required for a given application; thus, most such materials are used either as blends, alloys or composites. Further, the properties of a composite material depend not only upon the properties of the individual components, but also upon the composite's phase morphology and interfacial properties.[1]

In nature we know examples of organisms producing mineral–polymer composites with outstanding properties. The formation of these materials is highly regulated, showing typical structure characteristics on the nanometer and the micrometer scales, and is controlled by a polymeric matrix that acts as a spatially restrictive microenvironment and molecular template for inorganic mineralization.[2]

Nanostructured material can be prepared by different chemical methods in a variety of 'microvessels' or matrices mainly constituted by reverse micelles, liposomes or micro- and nano-porous organic and inorganic polymers.[3–5] The main functions of the matrix are: (a) acting as a templating agent during the reaction; (b) avoiding aggregation of the particles; and (c) possibly stabilizing the nanoparticles. It is now recognized that the confinement offered by these systems controls to a great extent the mechanical, magnetic and optical properties of the resulting material.[6]

Ziolo and coworkers[7,8] and Mauchessault and coworkers[9] have reported about γ-Fe_2O_3 nanoparticles prepared in a polystyrene-type ion-exchange resin and ferrites in cellulosics. Both these composites showed interesting results: in the first case as a magnetic material with appreciable optical transmission in the visible region (absorption coefficient below $10^4\,cm^{-1}$ throughout much of visible), and in the second case as a material exhibiting a high saturation magnetization (about $25\,J\,T^{-1}\,kg^{-1}$). We have further pursued the synthesis of these two classes of nanocomposites, preparing Fe_3O_4 nanoparticles in different ion-

* Correspondence to: L. Suber, ICMAT–CNR, Area della Ricerca di Roma, Via Salaria km 29,300, 00016, Monterotondo St., Rome, Italy.
E-mail: suber@mlib.cnr.it
† Based on work presented at the 1st Workshop of COST 523: Nanomaterials, held 20–22 October 1999, at Frascati, Italy.
Contract/grant sponsor: CRAFT; Contract/grant number: BE-S2-2806.

exchange resins and cellulosics. A detailed structural and morphological characterization of the composites is reported.

EXPERIMENTAL

Materials

The resins used are of the polystyrene type crosslinked with divinyl benzene: BIO-REX 63, Bio-Rad (labeled BR), and RD50w, Dowex (labeled RD).

The celluloses were: Powder P-10, Whatman (labeled CP) and Cellex-SE, Bio-Rad, (labeled CS). $FeCl_3$ and $FeCl_2$ salts were purchased by Aldrich and used as received; H_2O used is Water Plus for HPLC (Carlo Erba).

Instruments

The iron percent (w/w) of 5% nitric acid solutions was determined by means of a Perkin–Elmer Model 372 atomic absorption spectrophotometer. Transmission electron Microscope (TEM) measurements were performed with a Philips CM 20 operating at 200 kV. The samples were ground in ethyl alcohol and ultrasonicated; a drop was then deposited between two Formvar grids. Scanning electron microscope (SEM) measurements were performed with a Cambridge 360 equipped with an LaB_6 filament and a removable beryllium window. The scanning secondary and backscattered electron images were acquired operating at 20 kV and at a working distance (wd) of 25 mm for obtaining the energy dispersive spectra (EDS) and at a lower wd for the electron images. The samples were first dispersed in ethyl alcohol with one drop of collodion and then deposited in a graphite sample-holder in order to avoid any possible presence of elements other than those from the samples.

Thermogravimetric–differential thermal analysis (TG–DTA) measurements were carried out using STA 780 STANTON equipment under the following experimental conditions: heating rate, 5 °C min^{-1}; nitrogen flow rate, 70 ml min^{-1}.

Synthesis

The reactions were performed under a nitrogen atmosphere. Typically, 3 g of the matrix were reacted with an aqueous solution formed by 100 ml of 0.05 M $FeCl_3$ and 50 ml of 0.05 M $FeCl_2$, followed, after washing to eliminate excess Fe^{2+} and Fe^{3+} ions physisorbed on the matrix, by alkalinization with 120 ml of 0.1 N NaOH solution. The dark-brown products were washed several times with water and dried under vacuum.

RESULTS AND DISCUSSION

The syntheses of magnetite nanoparticles in ion exchange resins and cellulosics were performed in accordance with Scheme 1. Ion-exchange resins or celluloses, functionalized with PO_3^{3-}, SO_3^{2-} or PO_4^{3-} groups (A^-), are immersed in an Fe^{3+}/Fe^{2+} (ratio 2:1) chloride solution; their cations Na^+ or $H^+(C^+)$ are substituted by Fe^{3+} and Fe^{2+} ions; by hydrolysis and polymerization at 65 °C in an alkaline medium, magnetite nanoparticles are formed in the resin macropores or in the interstitial space of the swollen cellulose microfibers. The process can be repeated many times, loading the nanocomposite with more Fe_3O_4 nanoparticles.

It is interesting to examine how, using the same iron concentration and procedure, the matrix influences the formation of the iron oxide nanoparticles.

For the polystyrene type (crosslinked with divinyl benzene) we have used matrices with different functional groups and cations: (1) with

$$[\text{Matrix}\text{–}(A^- - C^+)_8]_n + n(2Fe^{3+} + Fe^{2+}) \xrightarrow{-n8C^+} [\text{Matrix}\text{–}(A^-)_6(Fe^{3+})_2(A^-)_2Fe^{2+}]_n$$

$$\uparrow \text{ recycling} \qquad \swarrow \text{NaOH, 65 °C}$$

$$[Fe_3O_4 \ @ \ \text{Matrix}\text{–}(A^- - Na^+)_8]_n$$

A^- = anion
C^+ = cation
@ = within

Scheme 1

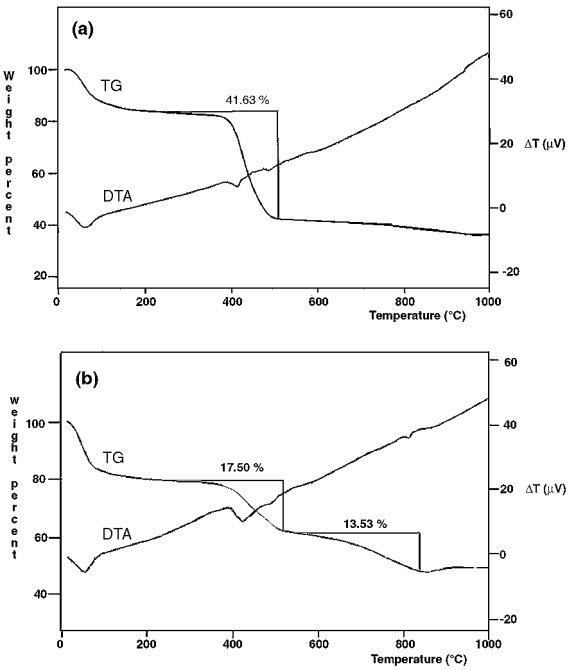

Figure 1 (a) TG and DTA curves of the polystyrene-type resin BR; (b) TG and DTA curves of the polystyrene-type BR/Fe_3O_4 nanocomposite.

$A^- = PO_3^{3-}$, $C^+ = Na^+$ (label BR); (2) with $A^- = SO_3^{2-}$, $C^+ = H^+$ (label RD).

The percentage of iron (w/w) found in the nanocomposites after one cycle, determined by atomic absorption spectrophotometry, is about 11% w/w for the RD samples and 3% w/w for the BR samples (to reach the 11% w/w of iron content, the BR nanocomposite needs to be recycled).

Figure 1a and b shows the TG–DTA curves of the resin and of the corresponding nanocomposite where the iron content is 11% w/w. A remarkable difference in weight loss is observed in the region 300–500 °C in the two cases. In fact, whereas a weight loss of *ca* 42% is observed in the resin, only a weight loss of about 17.5% is observed in the nanocomposite, indicating a higher thermal stability of the nanocomposite compared with its matrix.

Further, in Fig. 1b we observe, in the region between 500 and 800 °C, a weight loss of 13.53%, when added to the preceding loss of 17.50% this gives a total loss of 31.03%. Considering that the nanocomposite contains 11% (w/w) of iron, we should expect a weight loss of *ca* 35% (35.3% if the iron oxide is Fe_3O_4 and 35.1% if the iron oxide is Fe_2O_3). The difference of *ca* 4% between the theoretical (35.1%) and experimental (31.03%) values can be attributed to the oxygen uptake (possible also in a nitrogen atmosphere if it contains oxygen impurity) needed to transform magnetite to maghemite:

$$2Fe_3O_4 + 1/2O_2 \rightarrow 3Fe_2O_3 \text{ (theoretical: } + 3.4\% \text{ w/w)}$$

Structural and morphological investigations

Table 1 lists the most intense powder diffraction peaks of the reference samples Fe_3O_4 and γ-Fe_2O_3 and of the nanocomposites. Magnetite (Fe_3O_4) slowly oxidizes to maghemite (γ-Fe_2O_3), so it is very important to check by X-ray powder diffraction measurements the phase of the iron oxide. Unfortunately, this is not an easy task, as the powder diffraction data of the two phases are very similar.

In the case of the BR nanocomposite, Table 1 shows the powder diffraction data of the as-prepared sample (BRF) and of the sample after 72 h milling in air (BRFM). Comparing the data of the two samples, the peak values are different; whereas the BRF values are close to the magnetite values, the BRFM values are very close to the maghemite values. It is thus reasonable to suppose that the BRF sample contains magnetite, which in

Table 1 Most intense X-ray powder diffraction peaks (values in 2θ)

Magnetite, Fe_3O_4 (19-629 JCPDS)	*h k l*	Maghemite, γ-Fe_2O_3 (39-1346 JCPDS)	*h k l*	BRF	BRFM	RDF0	CPF	CSF
30.095	2 2 0	30.241	2 2 0	30.157			30.016	
35.423	3 1 1	35.631	3 1 1	35.321	35.550	35.641	35.582	35.204
43.053	4 0 0	43.284	4 0 0				43.407	43.135
53.392	4 2 2	53.734	4 2 2	53.279			53.060	53.030
56.944	5 1 1	57.273	5 1 1	56.875	57.398	57.236	56.627	56.527
62.516	4 4 0	62.926	4 4 0	62.565	62.718	62.944	62.919	62.656

air, after increasing the surface by milling, oxidizes to maghemite. On the contrary, the diffraction data of the as-prepared RD nanocomposite are close to those for maghemite. The different behavior can probably be attributed to the smaller average diameter of the magnetic nanoparticles in the RD nanocomposite compared with that for BR (see below). The decreasing of the average diameter, and thus increasing of the total surface, facilitates the oxidation process.

Finally, for the cellulose nanocomposites, the data are not clear. Probably in these cases, both phases are present in good percentages.

The ion-exchange resins used as matrices are commercial macroporous resins formed by beads of about 100–300 μm in diameter. Each bead is, in turn, constituted of microglobules; their interstitial space forms the macropores.[10]

Once the iron oxide nanoparticles are formed (see Scheme 1), the particles fill the 'free space' of the macropores. Owing to the importance that particle size and aggregation play in, for example, determining the magnetic behaviour of the nanocomposite, we examined the nanocomposites in detail by SEM and TEM.

Figure 2 shows a typical electron diffraction micrograph of iron oxide nanoparticles in the nanocomposites; the ring indicated is due to the reflections of the 440 crystallographic planes attributable both to the magnetite, and to the maghemite structure. It is, in fact, not an easy task to distinguish between the two iron oxide forms. The iron oxide nanoparticles in the BR nanocomposites are almost irregular spherical particles, showing an average diameter of 10 nm, as shown by TEM measurements (Fig. 3a). Smaller particles and a narrower size distribution are observed in the recycled BR nanocomposite (Fig. 3b).

Furthermore, SEM analyses of the same samples show the morphology of the resin. In particular, the micrograph in Fig. 4a shows a single spherical bead of about 120 nm in diameter. The micrograph in Fig. 4b compares the secondary and the backscattered electron images for the resin bead with the microglobules and the interstitial macropores. These latter images combined with the EDS results (not reported) allow one to identify the white particles as iron oxide phases. The secondary-electron image in Fig. 4c also discloses the presence of magnetite particles and aggregates on the fragment of the bead. As the macropores have diameters of about 500 nm, it is likely that those particles and aggregates of particles with a diameter less than 500 nm can fill the pores, whereas the

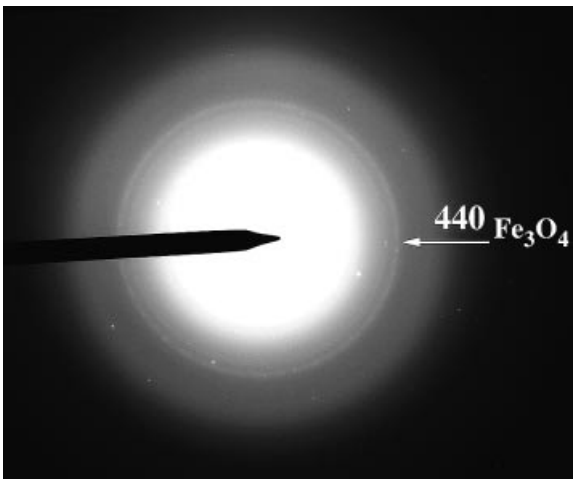

Figure 2 Electron diffraction micrograph of magnetite in the BR–resin nanocomposite.

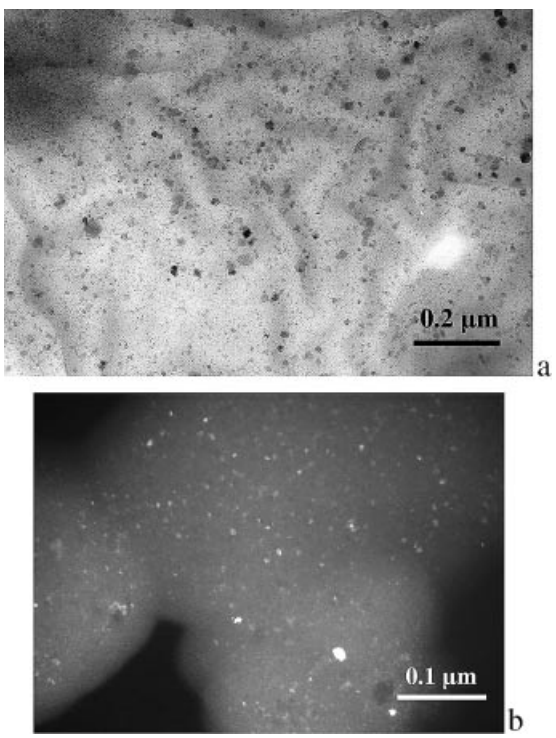

Figure 3 (a) Transmission electron bright-field micrograph of the magnetic particles contained in the BR–resin-type nanocomposites; (b) transmission electron dark-field micrograph of the magnetic particles contained in the BR–resin-type recycled nanocomposites.

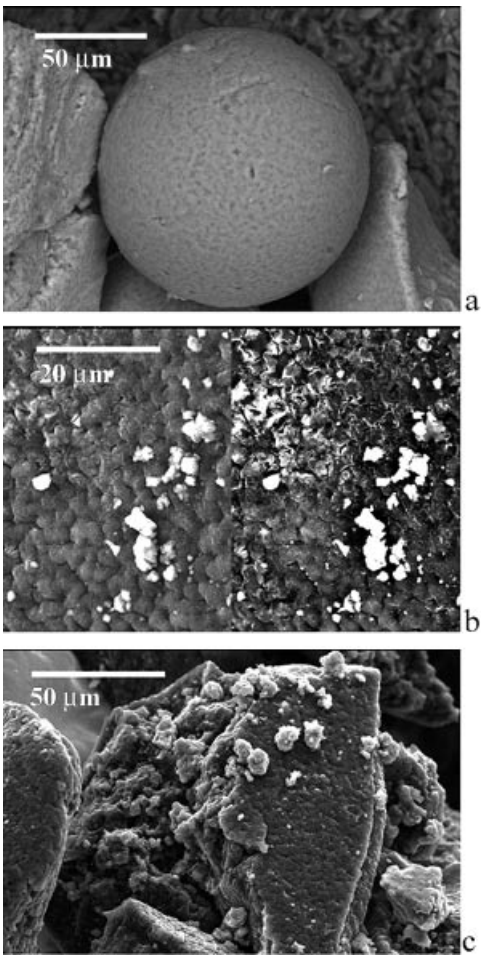

Figure 4 (a) Scanning backscattered electron micrograph of a BR-type resin bead; (b) scanning secondary (on the left) and backscattered (on the right) electron micrographs of the surface of a BR resin bead and magnetite particles and aggregates; (c) secondary-electron micrograph of a fragment of a BR resin bead and magnetite particles and aggregates.

larger aggregates remain on the surface of the beads. Neither the TEM nor the SEM measurements showed single iron oxide particles with a diameter greater than 30 nm. Furthermore, the EDS elemental analyses on the white grains showed that the grains were mainly constituted of iron and oxygen (with a very low percentage of sodium and phosphorus impurities originating from the resin). The Fe/O atomic ratio found, equal to 0.77, is comparable to the theoretical value of 0.75 for Fe_3O_4. These results, and the electron diffraction measurements (see above), suggest that, in our case, the iron oxide nanoparticles are consituted by

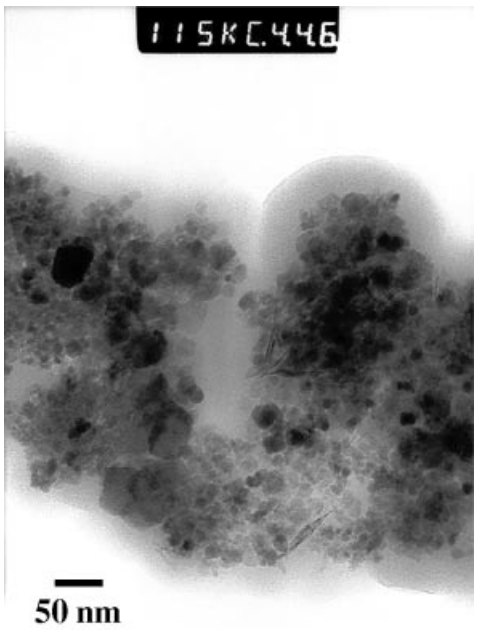

Figure 5 Transmission electron micrograph of the magnetite particles in the cellulose nanocomposite.

magnetite and not maghemite (Fe/O atomic ratio for γ-Fe_2O_3 equal to 0.67).

In the case of the RD composite, TEM measurements evidenced spherical magnetic particles with an average diameter (5 nm) smaller than in the preceding BR nanocomposite. In the case of the iron oxide–cellulose nanocomposites, TEM measurements show spherical magnetite particles of about 20–30 nm (Fig. 5).

Secondary- and backscattered-electron images for the cellulose are reported in Fig. 6 and show fibers of about 14 μm in width and 500 μm in length. Figure 7 shows secondary-electron images at a different magnification for the nanocomposites

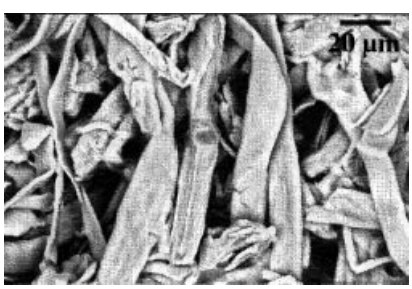

Figure 6 Scanning secondary-electron micrograph of the cellulose fibers.

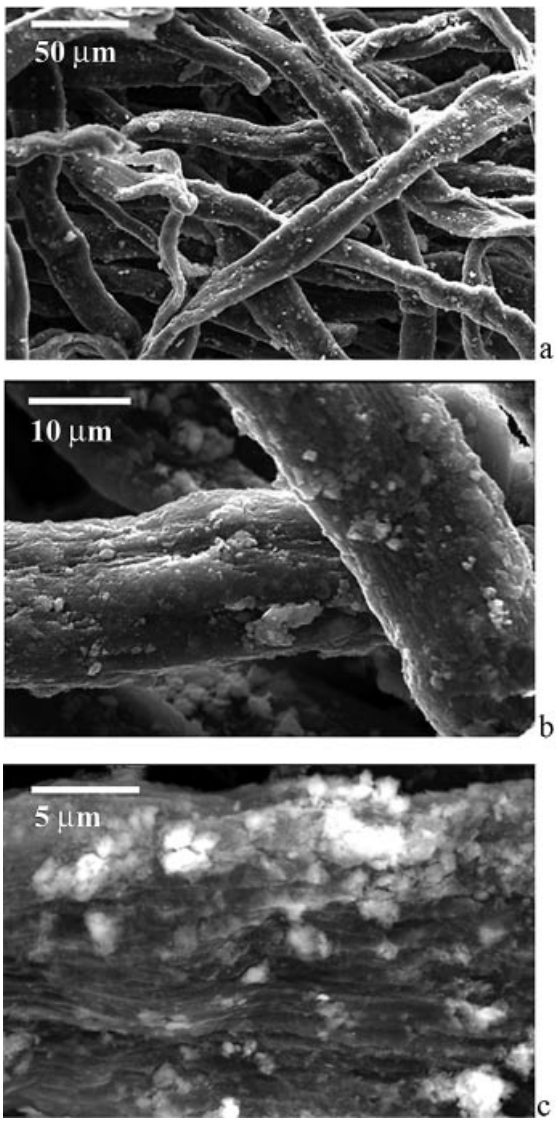

Figure 7 Scanning secondary-electron micrographs, at different magnifications, of the cellulose–iron oxide nanocomposite.

fibers that disclose the presence of iron oxide particles and aggregates on the surface of the fibers (Fig. 7a and b) and in the swollen network of the microfibers constituting the single fiber (Fig. 7c). The diameter of the almost-spherical particles is about 20–30 nm, and the aggregates on the surface of the fibers reach dimensions of about 2–5 μm.

Comparing the two classes of nanocomposites, one of the main differences is in the different average diameters of the magnetite particles: for the magnetite particles in the BR and RD resins this is 10 nm and 5 nm, respectively whereas in the cellulosics it is about 25 nm. It is likely that, under the same synthesis conditions, the swollen network of the microfibers in the cellulose allows more 'free space' for the growth of the particles compared with the micropores of the resins and/or the surface interaction between the organic and inorganic species plays a relevant role in the growth of the oxide.

CONCLUSIONS

The results obtained show that, starting from the same synthesis conditions for the preparation of magnetite nanoparticles, the confined spaces inside the matrices (the macropores in the case of the ion-exchange resins, and the interstitial space between the microfibers in the case of cellulose) influence the particle size. In fact, the magnetic nanoparticles are much smaller in the ion-exchange resin nanocomposites, where the macropores have diameters of about 500 nm, than in the cellulosics ones, where the swollen microfibers allow more free space for the growth of the particles. Anyway, in both cases, SEM measurements have shown aggregates of particles on the surface of the beads of the resin and on the surface of the fibers of the cellulose (see Figs 4c and 7b respectively) of a few micrometers, as also observed in the case of magnetic cellulose nanocomposites by Mauchessault and coworkers.[8] These results are important in order to understand fully the magnetic behavior of the nanocomposites.[11]

Acknowledgements This work was supported by the European Project CRAFT no. BE-S2-2806. The authors thank Mrs Cristina Riccucci for TG–DTA measurements, Mr Gianni Chiozzini for EDS–SEM measurements and Mr Saverio Alessandrini for technical assistance.

REFERENCES

1. Manson JA, Spelmer LH. *Polymer Blends and Composites*. Plenum: New York, 1976.
2. Mann S, Nebb J, Williams RJP (eds). *Biomineralization: Chemical and Biochemical Perspectives*. VHC: Weinheim, 1989.
3. Chen JP, Sorensen CM, Klabunde KJ, Hadjipanayis GC. *J. Appl. Phys.* 1994; **76**: 6316.

4. Mann S, Hannington JP, Williams RDP. *Nature* 1986; **324**: 565.
5. Ozeki S, Uchiyama H, Katada M. *Langmuir* 1994; **10**: 923.
6. Winnik FM, Morneau A, Ziolo R, Stöver HDH, Li WH. *Langmuir* 1995; **11**: 3660 and references cited therein.
7. Ziolo RF, Giannelis EP, Weinstein BA, O'Horo MP, Ganguly BN, Mehrotra V, Russell MW, Rayn DR, Huffman RH. *Science*, 1992; **257**: 219.
8. Raymond L, Revol J-F, Rayn DH, Mauchessault RH. *Chem. Mater.* 1994; **6**: 249.
9. Sourty E, Rayn DH, Mauchessault RH. *Chem. Mater.* 1998; **10**: 1755.
10. Suvec F, Fréchet JMJ. *Science*, 1996; **273**: 205.
11. Testa AM, Foglia S, Suber L, Fiorani D, Roig A, Casas L, Molins E, Grenéche JM, Tejada J. NATO ASI School, Magnetic storage beyond 2000. Submitted for publication.

